

MODELING OF ALUMINUM NANOPARTICLE FORMATION

R. Schefflan

D. Kalyon

S. Kovenklioglu

Stevens Institute of Technology

Highly Filled Materials Institute

Castle Point Station

Hoboken, N.J. 07030

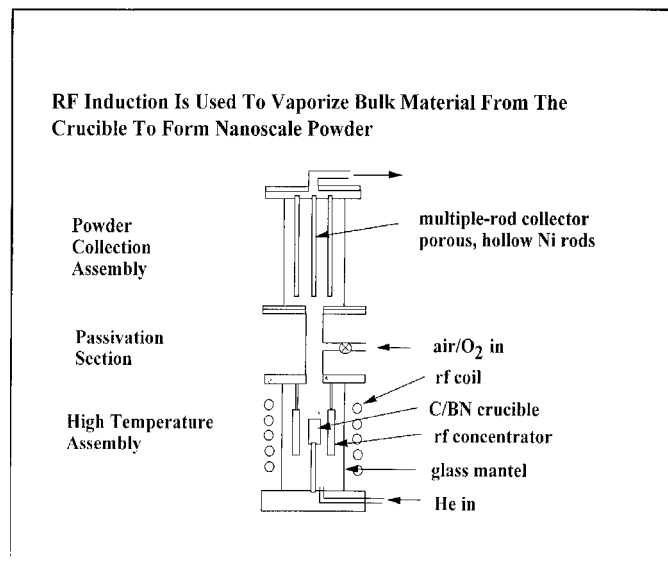
ABSTRACT

Picatinny Arsenal's process for making alumina coated nanoparticles of aluminum involves the conversion of gaseous aluminum, in the presence of helium carrier gas, to solid nanoparticles and their subsequent reaction with oxygen gas to form the oxide coating. Upon cooling, the aluminum precipitates to form solid nanoparticles. This part of the process can be described by the General Dynamic Equation for aerosols, which is the basis for mathematical modeling. The GDE was formulated as a set of numerical equations with particle volume and reactor holding time as the independent variables. The solution technique employs a set of numerical equations, which are solved explicitly. The solution requires that the integrals describing the ongoing coagulation processes be evaluated numerically at each grid point in the solution space. After all of the gaseous aluminum has solidified, a moment equation is employed to calculate the number of particles in each of the size distribution ranges.

INTRODUCTION

The effort to model the experimental aluminum nanoparticle reactor currently operating at the Picatinny Arsenal, shown in Figure 1, began in late 1999.

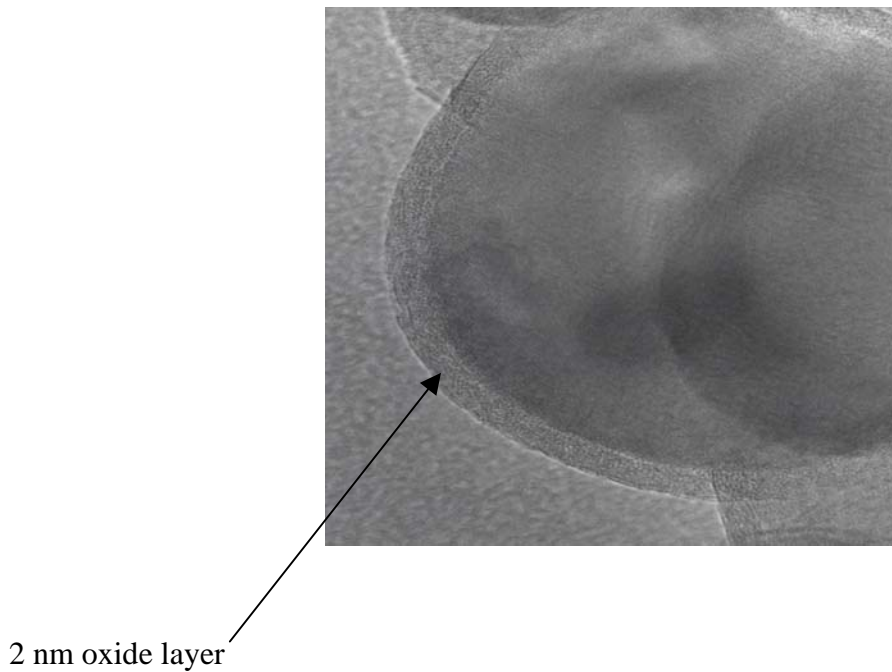
Figure 1. Picatinny Arsenal Experimental Reactor



The motivation to develop a mathematical model was based on the difficulty in developing an empirical scale-up of the process. Highly Filled Materials Institute personnel were able to see the reactor in operation. A few preliminary observations were made and data were collected so as to give direction to the modeling process.

The lab-scale process is carried out in a clear tubular reactor in which a plug of aluminum, located at the entry to the reactor, is heated with microwave energy such that aluminum gas is produced. The gas is continuously mixed with helium feed. Somewhere in the middle of the reactor, a second feed of oxygen gas is introduced. At this point all of the aluminum has solidified into nanoparticles. The oxygen reacts with the surface aluminum to form alumina. This passivates the nanoparticles. In this work the process for producing aluminum nanoparticles in the presence of helium carrier gas is modeled. Figure 2 depicts a sample of the reactor product seen under a scanning electron microscope

Figure 2. Scanning Electron Micrograph of an Aluminum Nanoparticle



METHODOLOGY

The basis of the calculations is the General Dynamic Equation (GDE)⁽¹⁾, which is a complete description of the aerosol dynamics in terms of a particle size distribution function and is given by Equation 1 below

$$\frac{\partial n}{\partial t} + \frac{\partial Gn}{\partial t} - I(v^*)\delta(v - v^*) = \frac{1}{2} \int_0^v \beta(v - V, V)n(v - V, t)n(V, t)dV \quad [1]$$

$$- n(v, t) \int_0^\infty \beta(v, V)n(V, t)dV$$

where n is the particles size distribution function, G is the growth law, v is the particle volume, $I(v^*)$ is the nucleation rate, the delta function following the $I(v^*)$ is a Dirac function and β is the collision frequency. Particle growth is by Brownian coagulation and is represented by the two integrals. The first integral accounts for formation of particles of size v by coagulation of smaller particles. The second integral accounts for the loss of particles of size v by coagulation with all other particles. The theory of Brownian Coagulation⁽²⁾ employs the collision frequency function given by Equation 2 below

$$\beta(v_i, v_j) = 2k_b \frac{T}{3\mu} \left[\frac{1}{v_i^{1/3}} + \frac{1}{v_j^{1/3}} \right] \quad [2]$$

where k_b is Boltzmann's constant, T is the temperature, and μ is the viscosity. Since the contact time has been observed to be extremely short we assume that growth G , is negligible.

The nucleation rate is determined from classical nucleation theory^(1,3) which describes the homogeneous nucleation of dilute mixture of solids or liquids from a gas. The theory suggests that clusters of monomers are held together by van der Waals forces. The nucleation rate is given by Equation 3 below

$$I = \left[\frac{p_1}{(2\pi m_1 k_B T)^{1/2}} \right] \left[\frac{2v_1 \sigma^{1/2}}{(k_B T)^{1/2}} \right] n_1 \exp \left[\frac{-16\pi v_1^2 \sigma^3}{3(k_B T)^3 (\ln S)^2} \right] \quad [3]$$

where p_1 is the partial pressure of aluminum, v_1 is the molecular volume, σ is surface tension, and S is the partial pressure of aluminum in the gas divided by its' vapor pressure. The clusters become stable at a critical size d_p^* , given by the Kelvin Equation shown below:

$$d_p^* = \frac{4\sigma v_1}{k_b T \ln S} \quad [4]$$

MODEL DEVELOPMENT

The solution to the GDE was developed as an explicit discretization of the partial differential equation. The solution space for the GDE is divided into a grid incremented in particle volume v , and contact time t . The contact time is calculated by dividing a discrete element of reactor volume by the flow rate of gas entering that element. Thus the solution develops by a repeated solution of a numerical version of the GDE at each element of reactor volume for all increments of particle size. The integrals on the right hand side of the equation are repeatedly evaluated, numerically, for use in the solution of the GDE. The explicit formulation was developed using a forward difference for the first term in the equation. The Nucleation Equation together with the Kelvin Equation are used to calculate the nucleation rate at each time step and the integrals calculated numerically at each step in particle volume. The complete formulation is given in numerical form as Equation 5 below:

$$n_{v,t+\Delta t} = n_{v,t} + \Delta t \left[I(v^*) \delta(v - v^*) + \frac{1}{2} INT_1 - n_{v,t} INT_2 \right] \quad [5]$$

where INT_1 and INT_2 represent the first and second integrals in the GDE.

The technique employed is to establish the grid size after which the numerical GDE is solved at each discrete value of v , particle size, at a specific t , time (which corresponds to an increment in reactor volume) within the grid. After all $n_{v,t}$ are calculated, a material balance is performed to establish the gas concentration for the next time step and to check that all of the aluminum has not been converted to particles at that particular time. The reactor volume is then incremented, the next time value calculated by reactor volume increment divided by entering gas flow rate and the entire process is repeated until no more aluminum is left in the vapor phase. When the GDE calculations end the last set of distribution function values are repeatedly integrated with respect to volume size, between each set of values ranging over 10 per cent of the volume size, for example between 40 and 50 percent of the full range of particle sizes. This is the first moment of the distribution function with respect to v and gives the number of particles in that size range and is shown below

$$N = \int_a^b n(v,t) dv \quad [6]$$

where, $n(v,t)$ represents the values of the distribution function at time t , varying between sizes a and b .

The numerical version of the GDE in conjunction with the various required analytical equations provides two possibilities:

1. Exploration of the process conditions to determine the initial particle size and the nucleation rate.
2. Calculation of the distribution function.

NUCLEATION CALCULATIONS

Identification of practical operating conditions was carried out by calculating nucleation rates and critical particle sizes for a variety of operating temperatures varying between 900 and 1200 °C and at pressures of 5 and 10mmHg at a constant vapor composition. Figure 3 shows the effects of temperature and pressure on the nucleation rate, Figure 4 shows their effects on critical particle diameter, and figure 5 shows their effects on supersaturation in the gas.

Figure 3 - Effect of Temperature and Pressure on Nucleation

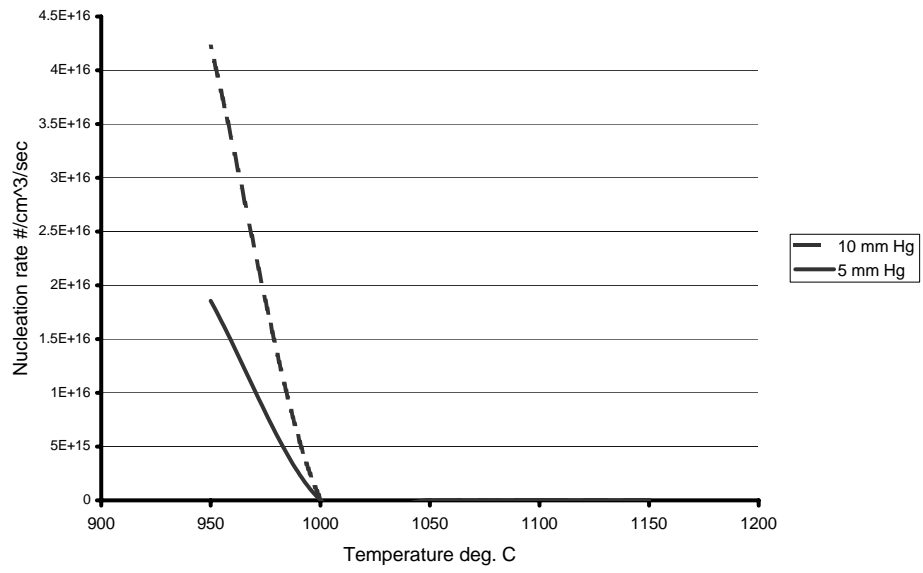


Figure 4. Effect of Temperature and Pressure on Critical Particle Size

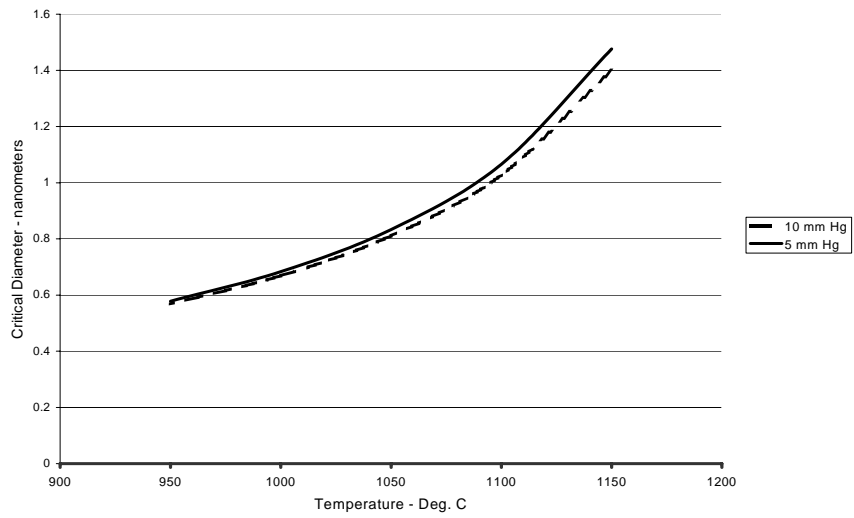
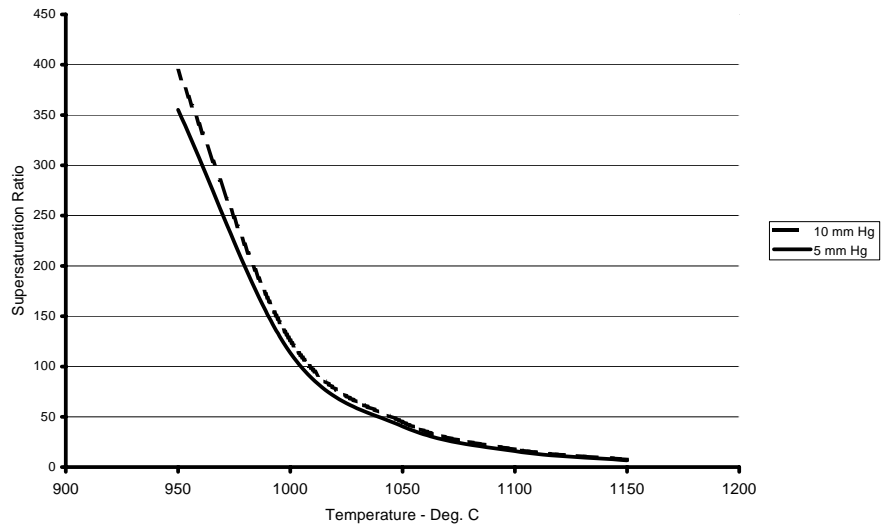


Figure 5. Effect of Temperature and Pressure on Supersaturation



DISTRIBUTION FUNCTION CALCULATIONS

For purposes of illustrating the ways that a solution could be employed a sample problem is illustrated here. The complete solution i.e. the matrix of solution space, is too large to show here however sample plots derived from the data are shown below. Figure 6 illustrates the distribution function at various reactor contact times expressed as tau, reactor volume divided by flowrate, Figure 7 shows the number of particles in 10 percent size range increments at the end of the run, and Figure 8 shows supersaturation, the driving force for particle formation, at various reactor contact times i.e. the partial pressure of metal in the gas relative to its' vapor pressure.

Figure 6. Particle Distribution Function at Various Contact Times

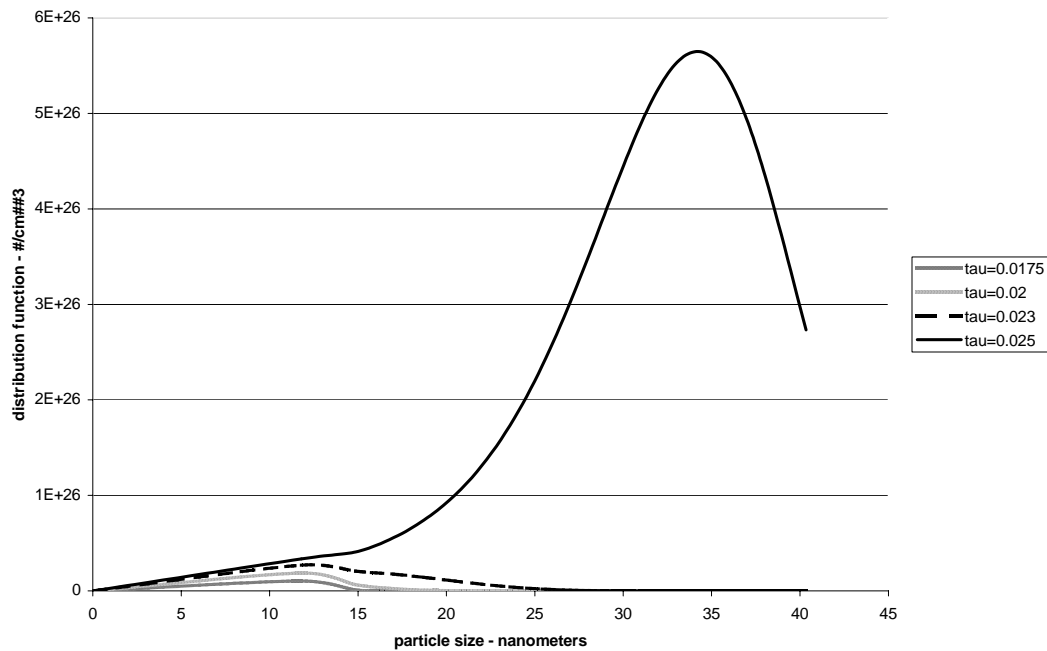


Figure 7. Number of Particles in Ten Percentile Ranges

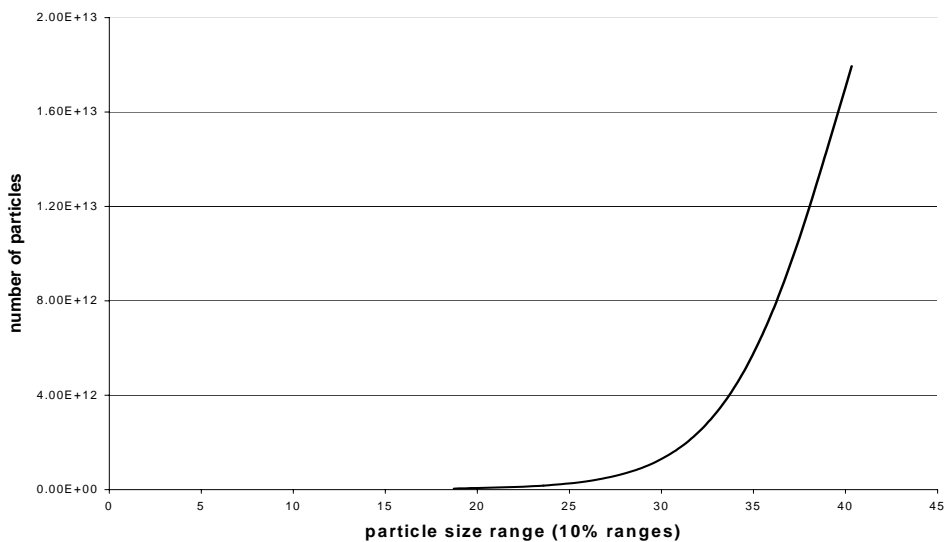
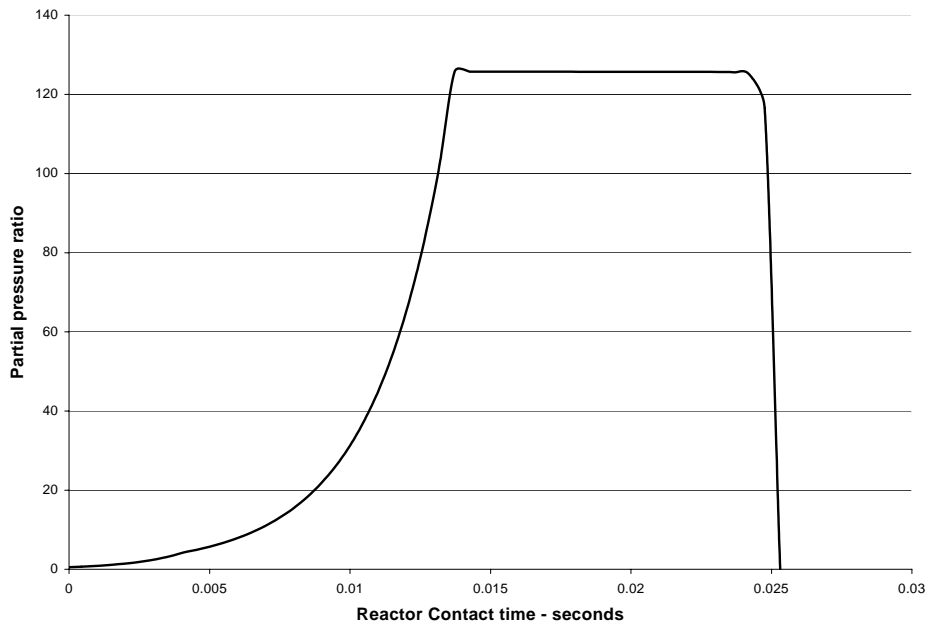


Figure 8. Effect of Gas Composition on Supersaturation



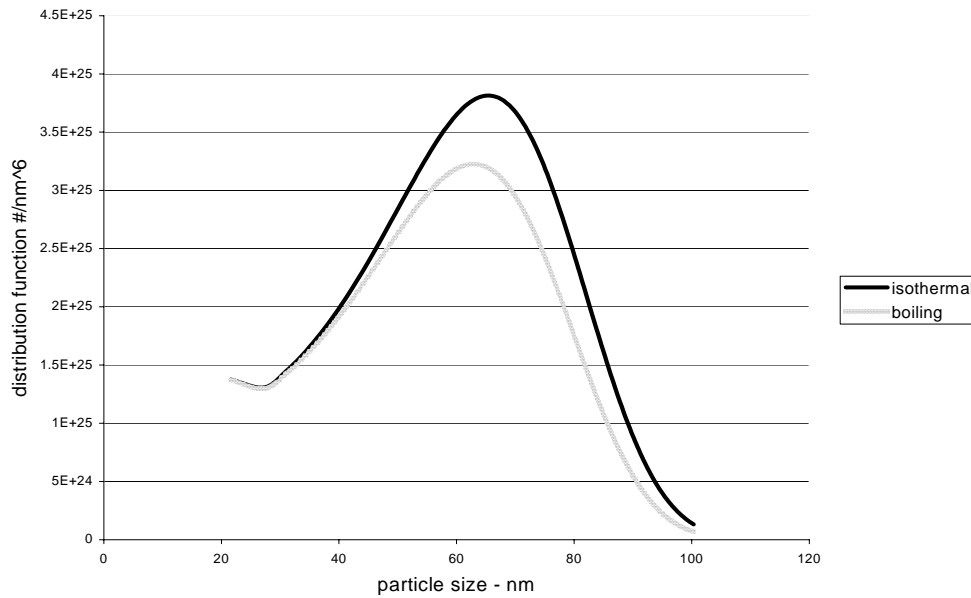
CASE STUDIES

At this moment in time there is very little experimental data to permit model validation. Qualitative observations such as the formation of a plume near the surface of the boiling aluminum, agree with the results of the calculations. The examples given below are invented for the purposes of illustrating the type of studies that could be undertaken.

1. Boiling or Temperature Controlled Liquid Metal Pool

Though the existing experimental system does not employ temperature control on the liquid metal pool, this is certainly feasible. Figure 9 below shows two comparable solutions one in which the material rapidly cools to the same temperature at which the second curve is controlled at. Initially the temperature of the boiling material is too high to form nuclei whereas in the temperature controlled calculation nuclei form immediately. This results in a delay of aerosol formation (57 reactor volume steps) in the boiling calculation relative to the one that is temperature controlled. There are also differences in the distribution function in that a greater number of particles of mean size are formed in the boiling case. Another difference is that the number of volume steps (of equal size) during which the aerosol is formed, required to bring the vapor to its saturated condition is considerably less (25 reactor volume steps) in the isothermal case than in the boiling case. The importance of these factors can only be evaluated in light of the process design, but the model can be used to focus attention on them.

Figure 9. Example 1 Comparisons

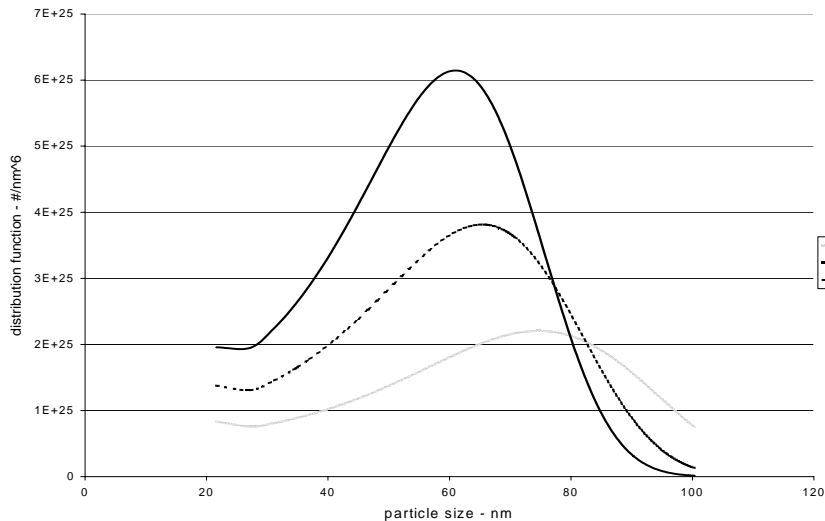


2. Effect of Pressure With Constant Temperature Distribution Along Length of Reactor.

System pressure has a pronounced effect on nucleation rate and critical particle size, see table below. A reduction in pressure produces a lower saturation ratio accompanied by a reduction in the nucleation rate. Figure 10 shows these effects on the system, with the lower pressure yielding a relatively wider range of particle sizes being produced with a larger mean particle size but fewer particles.

Pressure mmHg	Temperature deg. C	Saturation ratio	mole fraction vapor	Nucleation rate number/cm**3/sec
10	1025	134.01097	0.196601334	3.98805E+15
6	1025	118.48185	0.289698779	1.05672E+15
5	1025	111.993	0.328599557	5.5953E+14
4	1025	103.49121	0.379567979	2.22187E+14

Figure 10. Effect of Pressure on Distribution Function



3. Effect of Temperature Distribution Along Length of Reactor at Constant Pressure

Two constant pressure runs were made with the model while imposing two different temperature profiles on the system. Both employed an initial temperature of 1025 degrees Centigrade. The first run had a linear temperature profile imposed ending at about 700 degrees Centigrade near the reactor position at which all of the aluminum in the vapor phase had condensed. The second run employed a constant temperature of 1025 degrees Centigrade. The results are shown in Figures 11 and 12.

Figure 11. Isothermal

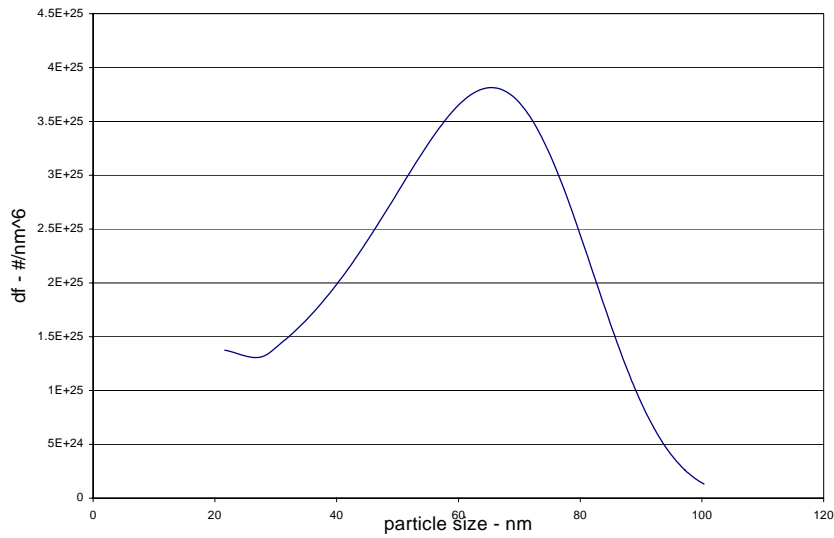
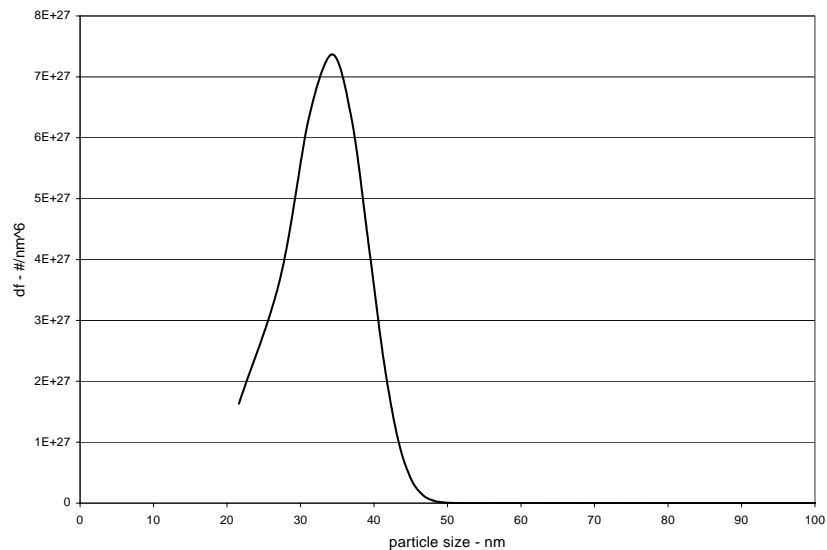


Figure 12. Linear Temperature Profile

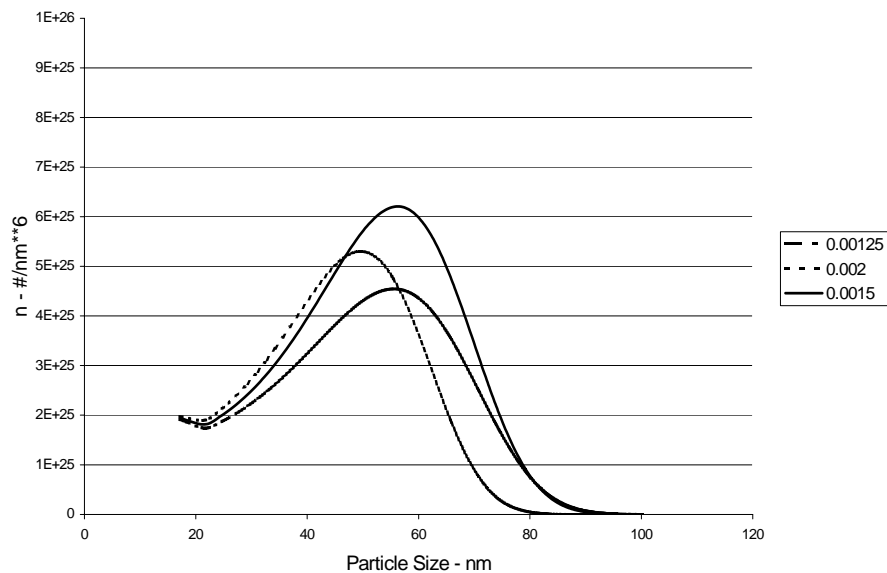


The results are pronounced as one may observe that the isothermal case yields a relatively wide particle size distribution ranging from about 30 to 100 nanometers with a mean of about 65 nanometers and distribution function values on the order of 10^{27} , whereas the imposed linear temperature profile produces a particle size distribution ranging from about 20 to 50 nanometers with a mean of about 35 nanometers and with distribution function values on the order of 10^{25} . Variations on these possibilities may be a means by which particle size distribution is controlled.

SOFTWARE STATUS

The solution technique employed in the program is an explicit equation similar to an Euler solution to a differential equation. Though this method provides no internal error control, the approximations to the derivatives improve as the step size decreases. Complicating factors which are difficult to assess involve the fact that two numerical integrations are performed at each step in particle size, and one integration is performed at each reactor volume step. It is important that users develop solutions, that are specific to their problem, at various step sizes to assure that they achieve a solution without excessive error. An example of the development of such a solution is given in Figure 13 in which the solution grid varied between 100x50 to 200x100. Here, the distribution function at the reactor volume step immediately prior to the disappearance of gaseous aluminum is plotted. Only the larger grids used are shown in the figure. It appears that the solutions are about the same and therefore acceptable.

Figure 13. Solutions at Different Grid Sizes



An implicit solution may be possible, however the complications due to the nested integrations as well as computer resources required to solve the resulting simultaneous equations, at each time step, appear prohibitive.

Examples of the types of data presentations were given above, but others can be guided by the user's imagination. For example, intermediate values of the number of particles within each size range can easily be developed .

ACKNOWLEDGMENTS

1. US Army TACOM/ARDEC for funding under DAAE30-97-D-1009 Task #12.
2. Professor M. Libera of Stevens Institute of Technology for Scanning Electron Microscope analysis.
3. Mr. M. Lang of Picatinny Arsenal for technical contributions.

REFERENCES

1. Friedlander, S.K. Smoke, Dust and Haze, New York: Wiley Interscience, 1977.
2. Hidy, G.M. & Brock, J.R. J. Colloid Science 20, 1965, 477-491.
3. Seinfeld, J.H. Atmospheric Chemistry and Physics of Air Pollution. New York: Wiley Interscience, 1986.